LIMNOLOGY
and
OCEANOGRAPHY: METHODS

ASLO

Limnol. Oceanogr.: Methods 00, 2016, 00–00

doi: 10.1002/lom3.10116

Application of membrane inlet mass spectrometry to measure aquatic gross primary production by the ^{18}O in vitro method

Sara Ferrón,*[1,2] Daniela A. del Valle,[†1,2] Karin M. Björkman,[1,2] Paul D. Quay,[3] Matthew J. Church,[1,2] David M. Karl[1,2]

[1]Daniel K. Inouye Center for Microbial Oceanography: Research and Education, University of Hawaii, Honolulu, Hawaii
[2]Department of Oceanography, School of Ocean and Earth Science and Technology, University of Hawaii, Honolulu, Hawaii
[3]School of Oceanography, University of Washington, Seattle, Washington

Abstract

The ^{18}O technique is considered the most direct in vitro method for measuring gross primary production (GPP) in aquatic ecosystems. This method measures the ^{18}O enrichment of the dissolved O_2 pool through photosynthesis after spiking a water sample with a tracer amount of ^{18}O-labeled water (^{18}O-H_2O) and incubating it under natural light conditions. Despite its advantages, the ^{18}O technique has only scarcely been used to measure GPP in the ocean. The lack of ^{18}O-based primary productivity measurements is most likely due to the technical difficulty associated with sample collection, handling, and processing, and to the need of an isotope ratio mass spectrometer (IRMS) for sample analysis, which is not available for the majority of research groups. The current procedure also precludes at sea measurements. In this manuscript, we demonstrate that the biological ^{18}O enrichment of dissolved O_2, after incubation of seawater enriched with ^{18}O-H_2O, can be precisely measured by shipboard or laboratory-based membrane inlet mass spectrometry (MIMS). The method was validated in the low-productivity oligotrophic North Pacific Subtropical Gyre, where the measured GPP ranged from 0.2 to 1.1 μmol O_2 L^{-1} d^{-1}, with an approximate precision for surface waters of ± 0.02 μmol O_2 L^{-1} d^{-1}. This new approach has the advantages of simple water sample handling and analysis, accurate dissolved gas measurements, capability of analysis on board of a ship, and use of relatively inexpensive instrumentation, and therefore has the potential to improve our understanding of primary production in the ocean and other aquatic environments.

Plankton photosynthesis in the surface ocean accounts for approximately 50% of the primary production on Earth (Field et al. 1998). It is a fundamental biochemical process as it affects the gas composition of the atmosphere by influencing air-sea fluxes of O_2 and CO_2 (Bekker et al. 2004), and plays a key role in the ocean carbon cycle (Volk and Hoffer 1985). It is also a critical ecological process as it represents the main source of energy and organic carbon into marine ecosystems, fueling food webs (Ryther 1969; Karl 2014).

Primary production in aquatic environments is usually determined by the production of dissolved O_2 or the incorporation of dissolved inorganic carbon into organic matter. The most common in vitro methods to measure phytoplankton photosynthesis include the oxygen-based light-dark bottle method (Gaarder and Gran 1927), the ^{14}C method (Steemann Nielsen 1952), and the ^{18}O in vitro method (Bender et al. 1987). Each of these methods has strengths and weaknesses, and all of them require an incubation period inside a bottle, which may alter the environmental conditions of the microbial community (Robinson and Williams 2005). The light-dark O_2 bottle method estimates net community production (NCP) and community respiration (CR) from changes in dissolved O_2 concentration in light and dark incubations, respectively, and gross primary production (GPP) is calculated from measured NCP and CR (Gaarder and Gran 1927). For oceanic measurements, this method relies on very small changes in dissolved O_2 concentrations superimposed over a large background, so GPP estimated by this methodological approach is subject to large uncertainty (Williams and Purdie 1991; Williams et al.

[†]Present address: Department of Chemistry and Biochemistry, University of Southern Mississippi, Hattiesburg, Mississippi
*Correspondence: sferron@hawaii.edu

2004). In addition, it assumes that respiration in the light equals respiration in the dark. The ^{14}C method estimates primary production from the incorporation of radioactive ^{14}C-labeled bicarbonate into organic matter (Steemann Nielsen 1952). Depending on the corrections made for dissolved organic matter production, grazing, and CR, this method yields a value between GPP and net primary production (NPP) (Pei and Laws 2014). The ^{14}C method is by far the most commonly used method for measuring primary productivity in the ocean and, even though the interpretation of ^{14}C uptake measurements may be ambiguous and the limitations of this technique have long been debated (Ryther 1955; Eppley and Sharp 1975; Peterson 1980; Dring and Jewson 1982; Bender et al. 1987; Marra 2002; Pei and Laws 2014), it is currently the standard method used to calibrate remote sensing algorithms (Behrenfeld and Falkowski 1997; Westberry et al. 2008). One of the limitations of the ^{14}C method is that a significant amount of the labeled particulate organic C may be re-mineralized to inorganic carbon or partitioned to the dissolved organic carbon (DOC) pool (Karl et al. 1998) by processes such as exudation, grazing, and/or viral lysis. Although the ^{14}C transferred to DOC can be measured, very few studies report it (Regaudie-de-Gioux et al. 2014; Viviani et al. 2015). The magnitude of the loss of ^{14}C-labeled particulate organic C depends on the length of the incubation relative to the growth rate of the organisms, the rate of respiration, and the rate of ^{14}C-DOC production; and thus, it is difficult to constrain. The ^{14}C uptake is thought to approximate GPP in short incubations (2–4 h) when respiratory losses are smaller, and net primary production in longer incubation times (~12 h) (Marra 2002). The ^{18}O in vitro method estimates GPP from the isotopic enrichment of dissolved O_2 as a result of the splitting of water through photosynthesis, after a tracer addition of ^{18}O-labeled water (^{18}O-H_2O) (Bender et al. 1987). This method provides a direct measurement of gross O_2 production that is not affected by respiratory processes or incubation duration, as the pool of dissolved O_2 is very large compared to respiration rates. Also, whereas the incorporated ^{14}C goes into different product pools, including dissolved and particulate organic matter, the labeled ^{18}O derived from the photosynthetic splitting of water is contained in a well defined product pool: dissolved O_2. An additional benefit compared to the ^{14}C method is that the tracer is not radioactive and, therefore, it is not regulated and/or restricted. Despite these advantages, and the fact that it is considered the most appropriate in vitro approach to measure oceanic GPP (Regaudie-de-Gioux et al. 2014), the ^{18}O method to date has not been as widely used as the ^{14}C method. The most likely reasons for this are that handling and analysis of samples for $\delta^{18}O$ analysis are technically difficult. Sample contamination with atmospheric air may also be an issue, and the measurement requires a specialized isotope ratio mass spectrometer (IRMS), which is not available for the majority of research groups, and even if it is, the IRMS needs to be specifically set up for the analysis of $\delta^{18}O$. In the one paragraph dedicated to the ^{18}O method, Falkowski and Raven (2007) state: "This technique allows a relatively precise measurement of gross photosynthesis; however, the method is tedious, requires a (bulky and expensive) mass spectrometer, and hence has not been widely used in studies of aquatic photosynthesis in nature."

In this manuscript, we propose the use of membrane inlet mass spectrometry (MIMS) to measure $\delta^{18}O$ in enriched samples. The main advantage of this approach is that it only requires a relatively inexpensive quadrupole mass spectrometer (QMS), which is small, easy to operate, and can be taken to sea for near real-time measurements of GPP. In addition, the sample handling and analysis are rapid and technically straightforward, and the dissolved gases are directly diffused from the water sample into the QMS, thus avoiding any gas extraction step that could introduce contamination (both during sampling and/or storage of samples). Here we validate the MIMS approach by comparing the values to those measured with the more conventional IRMS, and we present a number of in situ and on-deck incubation experiments from a low-productivity oceanic environment that further demonstrate its usefulness and general applicability.

Materials and procedures

Study site

Most of the experiments presented in this manuscript were conducted at Station ALOHA (22°45′N, 158°00′W), which is the site of the on-going Hawaii Ocean Time-series program (Karl and Lukas 1996; http://hahana.soest.hawaii.edu/hot/). Station ALOHA is located in the oligotrophic North Pacific Subtropical Gyre, a region of low chlorophyll concentrations, low photosynthetic activity and biomass, and very low nutrient concentrations (Karl and Church 2014). Due to their large areal coverage, the oligotrophic subtropical gyres play a key role in the oceanic global carbon cycle. However quantifying metabolic activity in these environments is very challenging due to low rates of primary production and respiration (Williams et al. 2004; Juranek and Quay 2005; Quay et al. 2010; Ferrón et al. 2015; Martínez-García and Karl 2015). In addition, the oligotrophic nature of the subtropical gyres makes incubation procedures complicated, as any contamination of trace amounts of nutrients or metals in the incubation vessels could have large effects on rate measurements (Fitzwater et al. 1982). Therefore, it is expected that validation of the MIMS method to measure GPP at Station ALOHA entails its applicability in other aquatic ecosystems, such as more productive oceanic sites, coastal zones, and freshwater inland ecosystems.

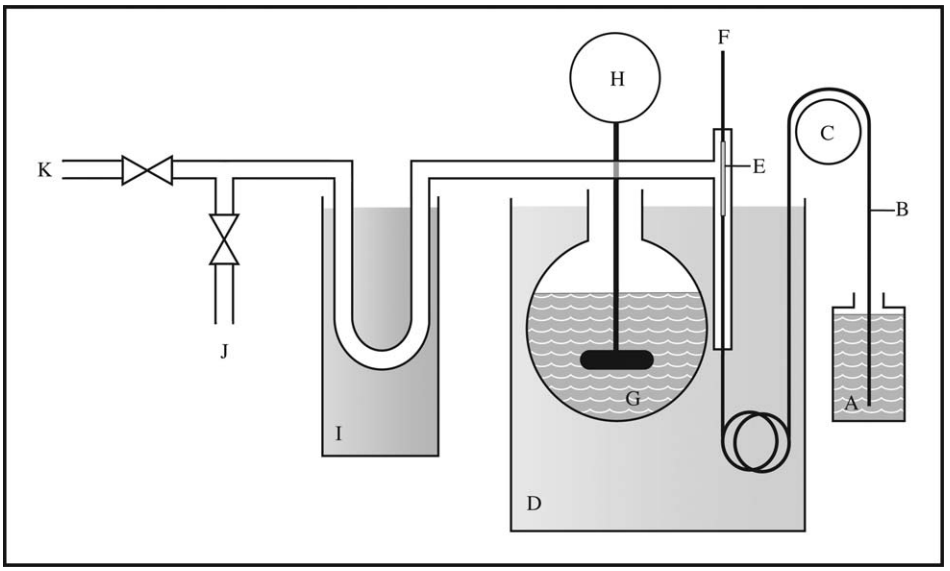

Fig. 1. Schematic of the membrane inlet setup (Bay Instruments, Easton, Maryland) connected to the QMS. The different components in the diagram are: sample vial (at least 12 mL in volume) (A), capillary tubing (B), peristaltic pump (C), 4-L water bath (D), silicone membrane (E), sample waste (F), flask containing the standard (G), stirrer to equilibrate the standard (H), 0.7 L liquid N_2 trap (I), connection to rough pump that creates vacuum before connecting the membrane inlet system to the QMS (J), and connection to QMS (K). The peristaltic pump (C) draws water from either the sample vial (as depicted in this diagram) or from the flask containing the standard (G). Components are not to scale.

Instrumentation

The relative abundance of dissolved $^{18}O^{16}O$ and $^{16}O^{16}O$ in seawater was measured by a MIMS dissolved gas analyzer (Bay Instruments, Easton, Maryland). The analyzer consists of a Pfeiffer Vacuum HiCube 80 Eco turbo pumping station connected to a HiQuad™ quadrupole mass spectrometer (QMG 700), with a Balzers radio frequency generator (QMH 400-5) and a Balzers analyzer (QMA 430). The latter is equipped with a cross-beam ion source, an 8 mm stainless steel rod system, a Faraday collector, and a 90° off-axis secondary electron multiplier (SEM).

The inlet design is described in detail by Kana et al. (1994) as modified in Kana et al. (2006), and depicted in Fig. 1. Briefly, a peristaltic pump (MiniPuls 3, Gilson) is used to pump the water sample at a constant flow (~2 mL min^{-1}) into capillary stainless steel tubing connected to Viton® pump tubing. The stainless steel tubing loops inside a water bath in order to stabilize the sample temperature to within 0.01°C. Inside the vacuum inlet the sample passes through a 2.5 cm long semipermeable microbore silicone membrane (Silastic®, DuPont) before exiting the vacuum. As the water flows through the membrane, a fraction of the dissolved gases are transferred from the water to the vacuum where they flow through a liquid nitrogen trap, which removes water vapor and carbon dioxide before entering the ion source in the QMS. The typical operating pressure inside the analyzer is $\sim 10^{-6}$ Torr. The ion currents for the data presented in this manuscript were measured using the SEM.

Sampling is done by inserting the stainless steel tubing to the bottom of the sample vial. Different size vials may be used. In this work, we used a range of 30–300 mL serum or glass vials with ground joint stoppers. The sample remains open to the air during the measurement, which takes approximately 3–5 min. This period is normally short enough that gas exchange with atmospheric air through diffusion is negligible. The length of time that the sample may remain open while sampling before contamination depends on the volume of the bottle, the depth to diameter ratio of the vial, and the concentration gradient (Kana et al. 1994).

For this study, mass to charge ratios (m/z) 28 ($^{14}N^{14}N$), 32 ($^{16}O^{16}O$), 34 ($^{18}O^{16}O$), and 40 (Ar) were normally recorded using the data analysis software Quickdata (Bay Instruments, Easton, Maryland). To account for drift in the signals during operation, a standard was run every 4–6 samples (~20–30 min). Based on the solubility equations of Hamme and Emerson (2004) for dissolved N_2 and Ar, and of García and Gordon (1992) for dissolved O_2, calibration factors were calculated for every standard run and interpolated with time (Kana et al. 2006). The isotopic composition of dissolved O_2 in the standards was calculated using the solubility fractionation reported by Kroopnick and Craig (1972). Typical variability in the calibration factors (measured as the coefficient of variation) over 4–8 h periods was ~2% for the individual signals, ~0.6% for O_2/Ar, and ~0.1% for $^{18}O/^{16}O$.

The standard consisted of filtered 25 m open ocean seawater (0.2 μm) of known salinity equilibrated with ambient air at 23.00°C (± 0.01°C). The standard was equilibrated in a 1-L round-bottom glass flask immersed in a temperature-controlled water bath for > 12 h, while mixing the water with a paddle attached to a stirrer (IKA lab Egg compact

mixer). The sample was also equilibrated to 23.00°C using the same water bath (Fig. 1). The relative humidity in the headspace was maintained at ~100% by covering the neck of the flask with a moist sponge. The selected temperature for the standard and the sample may be changed depending on the in situ temperature of the water samples (Kana et al. 1994, 2006).

Water sampling for incubation experiments

The seawater used during the different experiments was collected using standard 12-L Niskin-type bottles attached to a CTD rosette. The samples were taken from the Niskin bottles using powderless vinyl gloves, in acid-washed volume-calibrated Pyrex® or borosilicate glass bottles with ground-glass stoppers. The bottles were first rinsed with the seawater sample, and then filled from bottom to top using acid-washed silicon tubing, allowing the water to overflow at least twice the volume of the bottles. Before closing, the incubation bottles were spiked with ^{18}O-H_2O (97.2% ^{18}O, Medical Isotopes) by inserting the pipette tip below the neck of the bottle to ensure that the added ^{18}O-H_2O was not expelled when fitted with the stopper. The time-zero samples were stored in the dark until the start of the incubation, and then they were sub-sampled by siphoning into 40 mL crimp-sealed serum bottles and fixed with saturated mercuric chloride solution (~0.1% of the total sample volume) to inhibit biological activity. At the end of each incubation, the incubated bottles were processed identical to the time-zero samples, that is, sub-sampling into serum bottles and fixing with mercuric chloride.

Analysis of $^{18}O/^{16}O$ using IRMS

Samples for IRMS analysis were collected into pre-evacuated glass flasks poisoned with mercuric chloride and equipped with Louwers-Hapert valves (Bender et al. 1987; Emerson et al. 1999; Juranek and Quay 2005). The neck of each flask was flushed with ultra high purity N_2 before opening the valve. This is necessary to avoid contamination with atmospheric air by assuring that any bubble that accidentally enters the flask is O_2-free. While still flushing with N_2, the neck was filled with a small amount of water sample, the N_2 line was then removed, and all bubbles were eliminated by tapping the neck of the flask. Then, the valve was slowly opened, making sure to keep the water lock to avoid any air to enter the flask.

The isotopic composition of dissolved O_2 in the samples was determined using a Finnigan MAT 253 IRMS following the analytical procedure described by Juranek and Quay (2005).

Primary production measurements from ^{14}C-bicarbonate fixation

Rates of primary production determined using the ^{14}C incubation method (^{14}C-PP) were measured following Karl et al. (1996) and the HOT standard protocols (available at httphttp://hahana.soest.hawaii.edu/hot/protocols/protocols.html). Briefly, water samples were collected in triplicate directly from the Niskin bottles into 500 mL acid-washed polycarbonate bottles. Each bottle was spiked with ^{14}C-labeled bicarbonate (MPBiomedical #0117441H) to a final radioactivity of approximately 100 μCi L^{-1}, and incubated from dawn to dusk in a free-drifting array. After recovery, a small subsample was fixed in phenethylamine (Sigma-Aldrich #P6886) to measure the total radioactivity, and immediately thereafter the samples were filtered onto 25 mm glass fiber filters (Whatman GF/F).

Determination of GPP

The oxygen isotope ratio, ^{18}R, was determined as follows:

$$^{18}R = \frac{^{18}O}{^{16}O} = \frac{m/z\ 34}{(2\times m/z\ 32)+m/z\ 34} \quad (1)$$

The oxygen isotopic composition was expressed in δ-notation (McKinney et al. 1950), $\delta^{18}O$, which represents the abundance (in parts per thousand) of the isotope ^{18}O relative to its abundance in a reference standard:

$$\delta^{18}O = \left[\frac{R_{sample}}{R_{reference}} - 1\right]\times 1000 \quad (2)$$

For water, we express the $\delta^{18}O$ relative to the Vienna Standard Mean Ocean Water (VSMOW). For dissolved O_2, the $\delta^{18}O(O_2)$ at the end of an incubation is typically expressed relative to the value at time zero.

GPP was determined based on the change in the isotope ratio of dissolved O_2 over the incubation interval (^{18}O-GPP) (Bender et al. 1987, 1999):

$$^{18}O\text{-GPP} = \left[\frac{^{18}R(O_2)_{final} - ^{18}R(O_2)_{initial}}{^{18}R(H_2O) - ^{18}R(O_2)_{initial}}\right]\times[O_2]_{initial} \quad (3)$$

where $^{18}R(O_2)_{initial}$ and $^{18}R(O_2)_{final}$ represent the initial and final isotope ratios for dissolved O_2, $[O_2]_{initial}$ is the initial dissolved O_2 concentration, and $^{18}R(H_2O)$ is the isotope ratio of the incubation water, which is calculated based on the amount of ^{18}O-H_2O added and the calibrated volume of the incubation flask. For dawn to dusk experiments, Eq. 3 provides ^{18}O-GPP in μmol O_2 L^{-1} d^{-1}, as there should not be any splitting of water at night (Bender et al. 1987). For shorter incubations, the result of Eq. 3 was divided by the incubation time to get an hourly rate.

Determination of CR and NCP

The net oxygen change (NOC) over the incubation period can be simultaneously determined from the net change in O_2/Ar (Bender et al. 1999):

$$NOC = \left[\frac{(O_2/Ar)_{final}}{(O_2/Ar)_{initial}} - 1\right]\times[O_2]_{initial} \quad (4)$$

where $(O_2/Ar)_{initial}$ and $(O_2/Ar)_{final}$ are the initial and final O_2/Ar ratios. If it is assumed that photosynthesis and

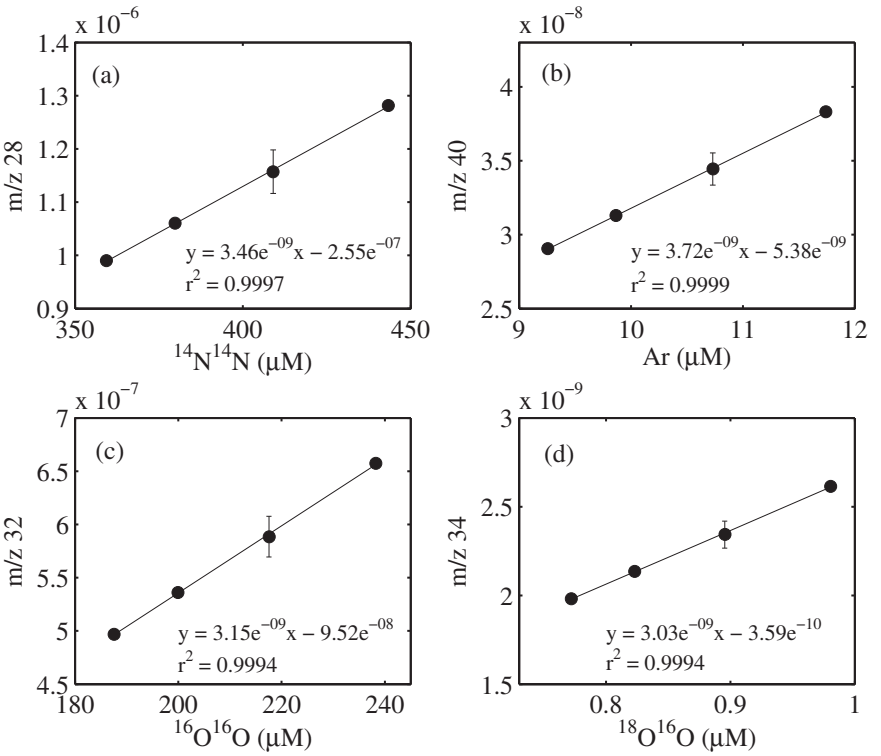

Fig. 2. Relationships between the mean QMS signal and the expected standard concentration for: (a) $^{14}N^{14}N$ or m/z 28, (b) Ar or m/z 40, (c) $^{16}O^{16}O$ or m/z 32, and (d) $^{18}O^{16}O$ or m/z 34. The line represents the linear regression between the mean QMS signal and the expected concentration. Error bars represent the SD of multiple samples ($n > 20$).

respiration are the only two processes affecting the O_2/Ar in the incubation bottle, and that the rate of respiration is constant throughout the day, then CR (μmol O_2 L^{-1} d^{-1}) can be estimated:

$$\mathrm{CR} = \frac{[^{18}\mathrm{O\text{-}GPP} - \mathrm{NOC}]}{\Delta t} \quad (5)$$

where Δt is the incubation time (days). Similarly, based on the same assumptions NCP (μmol O_2 L^{-1} d^{-1}) can be determined as:

$$\mathrm{NCP} = {}^{18}\mathrm{O\text{-}GPP} - \mathrm{CR} \quad (6)$$

Statistical analysis

To compare different sets of samples a one-way analysis of variance (ANOVA) and a significance level of $p < 0.05$ was employed.

Assessment

MIMS performance

The linearity of the MIMS response to different gas concentrations was tested for m/z 28 ($^{14}N^{14}N$), m/z 32 ($^{16}O^{16}O$), m/z 34 ($^{18}O^{16}O$), and m/z 40 (Ar). Standards consisted of 25-m filtered seawater (0.2 μm) collected at Station ALOHA and air-equilibrated to different temperatures: 18.0 (±0.1), 23.00 (±0.01), 28.0 (±0.1), and 32.0 (±0.1) °C (see Instrumentation section). The salinity of the standards was 35.464.

For the range of concentrations tested, the QMS responded linearly to m/z 28, 32, 34, and 40 (Fig. 2). It is important to note that all the values of m/z 28, 32, 34, and 40 from the experiments presented in this manuscript fall within the range of those plotted in Fig. 2, including those of ^{18}O enriched samples. Precision and accuracy results of four temperature standards are presented in Table 1. For measurements of dissolved N_2, Ar, O_2, and $^{18}O^{16}O$ concentration, the coefficient of variation (CV) for the four temperature standards averaged 0.16% for N_2 and 0.13% for the other gases. The CV of O_2/Ar and $^{18}O/^{16}O$ averaged 0.05% and 0.04%, respectively. Measured concentration values were all within 1.8% of the expected value, with an average of 0.9%. O_2/Ar ratios in the standards were within 0.4% of expected values, and $^{18}O/^{16}O$ ratios within 0.1%.

For surface seawater samples with ambient concentration values ($n = 5$), the reproducibility was ± 0.01% for O_2/Ar, ± 0.03% for $^{18}O/^{16}O$, and averaged ± 0.43% for the dissolved gases (Ar, O_2, and $^{18}O^{16}O$). The standard deviation (SD) of $\delta^{18}O(O_2)$ for the ambient seawater samples was ± 0.3‰, and ± 0.4‰ for the standards. These results demonstrate high precision through the whole sampling procedure.

Table 1. Precision and accuracy of dissolved gas analysis of seawater evaluated on temperature standards of known salinity. The instrument was calibrated with the 23.0°C standard.

	Temperature (°C)			
	18.0	**23.0**	**28.0**	**32.0**
N_2				
Mean (μM)	440.0	409.2	384.3	365.0
CV (%)	0.17	0.09	0.12	0.26
Expected (μM)	443.3	409.0	379.8	359.4
Δ(%)*	−0.75	0.04	1.17	1.55
O_2				
Mean (μM)	236.8	217.6	202.6	190.8
CV (%)	0.08	0.05	0.12	0.26
Expected (μM)	239.2	218.5	200.8	188.3
Δ(%)*	−0.99	−0.40	0.90	1.29
Ar				
Mean (μM)	11.65	10.73	9.92	9.32
CV (%)	0.11	0.05	0.11	0.25
Expected (μM)	11.74	10.73	9.87	9.26
Δ(%)*	−0.82	0.01	1.06	1.28
O_2/Ar				
Mean	20.42	20.36	20.40	20.43
CV (%)	0.05	0.01	0.09	0.05
Expected	20.37	20.36	20.35	20.34
Δ(%)*	0.24	0.00	0.25	0.42
$^{18}O^{16}O$				
Mean (μM)	0.97	0.90	0.83	0.79
CV (%)	0.08	0.08	0.11	0.27
Expected (μM)	0.98	0.90	0.82	0.77
Δ(%)*	−0.66	0.02	1.41	1.84
$^{18}O/^{16}O$				
Mean (‰)**	2.052	2.054	2.055	2.056
CV (%)	0.05	0.03	0.04	0.04
Expected (‰)**	2.054	2.054	2.053	2.053
Δ(%)*	−0.08	0.01	0.10	0.13

*The percent deviation (Δ) was calculated as the difference between the measured and expected value divided by the expected value and multiplied by 100.
**Note units in per mille.

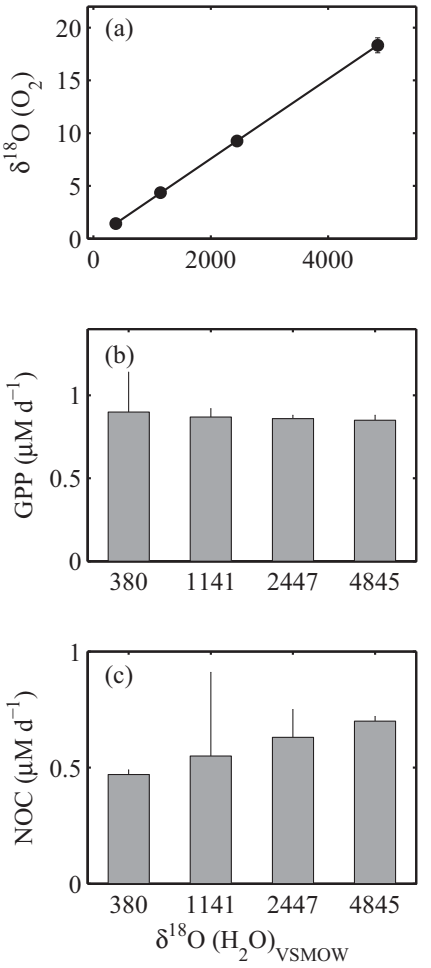

Fig. 3. (a) Relationship between the isotopic water enrichment relative to VSMOW, $\delta^{18}O(H_2O)_{VSMOW}$, and the final enrichment of dissolved O_2 relative to time zero. The $\delta^{18}O$ values are in ‰. The black line is a linear regression to the data ($y = 0.0038x + 0.0163$; $r^2 = 0.9999$). Calculated (b) GPP and (c) NOC for the different water enrichment experiments. Error bars represent one SD of triplicate samples, except for the smallest enrichment in which we had only duplicates.

Final $\delta^{18}O(O_2)$ and GPP as a function of initial water enrichment

In order to decide the minimum initial ^{18}O-H_2O enrichment needed to obtain a measurable enrichment in dissolved O_2 at Station ALOHA and also to check the potential negative or positive effects of the addition of ^{18}O-H_2O due to accompanying contaminants or nutrients, we measured ^{18}O-GPP adding different volumes of ^{18}O-H_2O. This experiment was conducted aboard the R/V *Kilo Moana* during a 5-d oceanographic cruise (HOE-Legacy 1, April 2015). The seawater was collected from a depth of 25 m and dispensed into 130-mL glass bottles with ground-glass stoppers. Triplicate incubation bottles were spiked with different volumes (100–1300 μL) of stock ^{18}O-H_2O to final enrichments of ~380, 1140, 2445, and 4845‰, and incubated from dawn to dusk inside an on-deck flow-through incubator that reproduces the in situ temperature and light field.

Fig. 3a shows that the $\delta^{18}O(O_2)$ values measured at the end of the incubation were significantly correlated ($r^2 = 0.9999$) with the initial water enrichment, corresponding to the different amounts of ^{18}O-H_2O added. The results show that even the smallest addition (~380‰ enrichment), resulted in a measurable enrichment of ^{18}O in dissolved O_2, that is, the final measured $^{18}R(O_2)$ after the incubation was significantly larger ($p < 0.01$) than the value at time zero. The GPP rates calculated for the different enrichments were not significantly different (Fig. 3b; Table 2), and the variability of the mean values was ± 3%. This indicates that with the

Table 2. Final $\delta^{18}O(O_2)$ relative to time-zero and GPP values (mean ± SD) measured for the different enrichments. Also shown is the estimated uncertainty of GPP values (see text).

^{18}O-H_2O (μL)	$\delta^{18}O(H_2O)_{VSMOW}$* (‰)	$\delta^{18}O(O_2)$ (‰)	GPP (μmol O_2 L^{-1} d^{-1})	Uncertainty (μmol O_2 L^{-1} d^{-1})
100	380 ± 6	1.4 ± 0.4	0.90 ± 0.24	±0.15
300	1141 ± 9	4.4 ± 0.2	0.88 ± 0.05	±0.05
650	2447 ± 89	9.2 ± 0.2	0.86 ± 0.02	±0.02
1300	4845 ± 20	18.3 ± 0.7	0.85 ± 0.03	±0.01

*The variability (SD) of $\delta^{18}O(H_2O)_{VSMOW}$ is due to differences in volume between the different bottles.

Table 3. Rates of ^{14}C-PP (μmol C L^{-1} d^{-1}) measured in situ during HOT 272 at Station ALOHA with and without the addition of ^{18}O-H_2O.

Treatment	Depth (m)	$\delta^{18}O(H_2O)$ (‰)	^{14}C-PP*
Control	25	0	0.50 ± 0.08
^{18}O-H_2O spiked	25	~2600	0.45 ± 0.08
Control	75	0	0.32 ± 0.03
^{18}O-H_2O spiked	75	~5230	0.33 ± 0.06

*Mean ± SD of triplicate measurements.

amounts used, the addition of ^{18}O-H_2O did not appear to enhance or diminish photosynthesis, unless a critical stimulatory or inhibitory threshold was reached with the lower dose. This is unlikely because, as shown in the next section, the addition of ^{18}O-H_2O did not stimulate or inhibit ^{14}C uptake. On the other hand, the NOC during the incubation, although not significantly different between the treatments, showed larger variability: ± 17% (Fig. 3c). The standard deviations of replicate samples for ^{18}O-GPP and NOC were not correlated, indicating that the source of variability may differ between both measurements.

In order to select the optimal enrichment it is important to note that whereas the $\delta^{18}O(O_2)$ values did not differ between the treatments, the uncertainty in the calculated GPP value decreased when increasing the final $^{18}R(O_2)$ (Table 2). The uncertainty in GPP was estimated by propagating the errors in the different terms of Eq. 3. The uncertainty in $^{18}R(O_2)$, σ_{18R}, and in dissolved O_2 concentration, σ_{O2}, were considered to be the SD of the replicate time zero samples ($n = 4$), that is, ± 0.36 × 10^{-3} ‰ and ± 0.7 μM O_2, respectively. The uncertainty in $^{18}R(H_2O)$ was assumed to be negligible. This way the uncertainty in GPP, σ_{GPP}, was estimated as follows:

$$\sigma_{GPP} = \left[\left(\frac{\sqrt{2}\sigma_{18R}}{{}^{18}R(O_2)_{final} - {}^{18}R(O_2)_{initial}} \right)^2 + \left(\frac{\sigma_{18R}}{{}^{18}R(H_2O) - {}^{18}R(O_2)_{initial}} \right)^2 + \left(\frac{\sigma_{O2}}{[O_2]_{initial}} \right)^2 \right]^{\frac{1}{2}} \times GPP \quad (7)$$

It is clear from Eq. 7 that an increment in $^{18}R(O_2)_{final}$ and $^{18}R(H_2O)$ will decrease σ_{GPP}. In this experiment, the estimated σ_{GPP} varied from 0.01 to 0.15 μM O_2 d^{-1} depending on the initial water enrichment, which represented between 2% and 20% of the GPP value. It is therefore important to find a balance between adding sufficient ^{18}O-H_2O to minimize σ_{GPP}, while keeping the addition small enough to minimize cost. For surface waters at Station ALOHA, an initial enrichment of ~2500‰ was considered appropriate, and resulted in an approximate uncertainty in GPP of ± 0.02 μmol O_2 L^{-1} d^{-1} (Table 2).

Effect of ^{18}O-H_2O additions on ^{14}C uptake

Because of the oligotrophic conditions at Station ALOHA, it is important to make sure that the addition of the tracer does not negatively or positively affect photosynthesis. To assess this we conducted ^{14}C uptake incubations in situ at two representative depths, 25 m and 75 m, together with the primary production depth-profile conducted during HOT 272. Triplicate samples were collected following HOT standard procedures for water collection. Samples were collected in acid-washed 75 mL polycarbonate bottles, and half of them were used as controls (i.e., no added ^{18}O-H_2O) while the rest were spiked with ^{18}O-H_2O. Based on the initial enrichments used in the vertical GPP profiles (see below), the 25 m samples were spiked with 400 μL of ^{18}O-H_2O (final enrichment of ~2600‰) and the 75 m samples were spiked with 800 μL of ^{18}O-H_2O (final enrichment of ~5230‰). Immediately after, all samples, including controls, were spiked with ^{14}C-bicarbonate, and incubated in situ from dawn to dusk in a free-drifting array.

Primary production rates, measured as ^{14}C uptake, were not significantly different in the control and ^{18}O-H_2O spiked samples (Table 3). For the two depths tested, 25 m and 75 m, the addition of ^{18}O-H_2O to a final water enrichment of ~2600‰ and 5230‰, respectively, did not significantly alter ^{14}C uptake rates. The water enrichments tested were similar to those used for the surface (5, 25, and 45 m) and deeper (75 and 100 m) in situ incubations, respectively, indicating that the amount of tracer used during the primary production depth profiles at Station ALOHA was appropriate and did not affect photosynthetic rates.

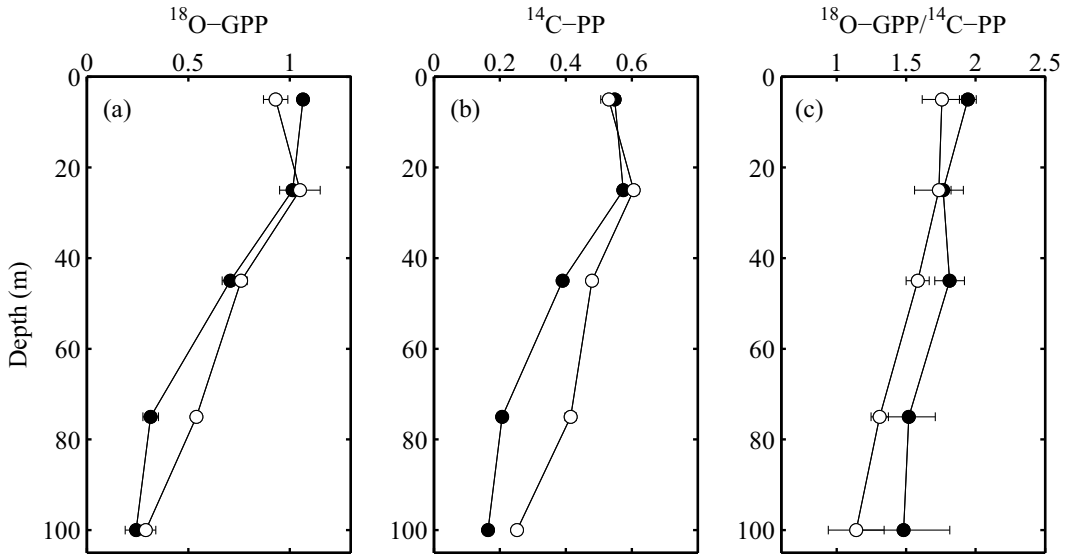

Fig. 4. Two depth profiles of in situ primary production rates measured at Station ALOHA using: (a) the ^{18}O in vitro method (units in μmol O_2 L^{-1} d^{-1}), and (b) the ^{14}C uptake method (units in μmol C L^{-1} d^{-1}). Also shown (c) the ratio of ^{18}O-GPP to ^{14}C-PP (mol O_2/mol C). Black and white circles represent profiles conducted on 07 April 2015 (HOE-Legacy 1) and 23 May 2015 (HOT 272), respectively. The error bars in (a) and (b) represent the SD of triplicate samples, whereas in (c) they represent the propagated error.

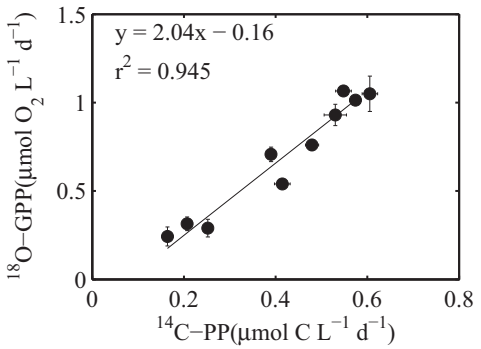

Fig. 5. Relationship between ^{18}O-GPP rates measured using MIMS and ^{14}C-PP. The data are from the two depth profiles conducted at Station ALOHA and shown in Fig. 4. The line is a model II regression fit to the data.

Primary production depth profiles at Station ALOHA

To validate the applicability of the MIMS for quantifying GPP via the ^{18}O in vitro method (^{18}O-GPP) in the oligotrophic oceanic site Station ALOHA, we measured ^{14}C-PP and ^{18}O-GPP rates in situ at different depths using a free drifting array during two cruises on the R/V *Kilo Moana*: HOE-Legacy 1 (April 2015) and HOT 272 (May 2015). The samples for ^{14}C-PP and ^{18}O-GPP were collected in triplicate from the same nighttime hydrocast and incubated at the same standard depths as HOT ^{14}C-PP depths: 5, 25, 45, 75, and 100 m. For ^{18}O-GPP determination, the incubation bottles were collected in 130 mL glass bottles with ground-glass stoppers. The incubation bottles were spiked with ^{18}O-H_2O and maintained in the dark until the deployment in the drifting array, at which time the time-zero samples were fixed with saturated mercuric chloride solution. Samples were incubated from dawn to dusk. The initial enrichment was ~2560‰ for the incubations at 5, 25, and 45 m, and ~5120‰ for incubations at 75 and 100 m. During HOE-Legacy 1, an extra set of triplicate samples with no addition of ^{18}O-H_2O was incubated in parallel with the enriched bottles to determine the effect of the addition of ^{18}O-H_2O on NOC.

The two depth profiles of ^{18}O-GPP and ^{14}C-PP rates conducted at Station ALOHA are shown in Fig. 4. As expected, elevated production rates were observed in the top 25 m of the water column, ranging from 0.7 to 1.1 μmol O_2 L^{-1} d^{-1} for ^{18}O-GPP, and from 0.4 to 0.6 μmol C L^{-1} d^{-1} for ^{14}C-PP. At 75 and 100 m, rates ranged from 0.2 to 0.5 μmol O_2 L^{-1} d^{-1} and from 0.2 to 0.4 μmol C L^{-1} d^{-1}, respectively. Measured rates of ^{18}O-GPP and ^{14}C-PP were positively correlated (Fig. 5, $r^2 = 0.945$), indicating that the ^{18}O-GPP measurements tracked the changes in primary productivity as determined by the ^{14}C uptake. The slope of a model II regression fit to the data was 2.0 ± 0.2 μmol O_2/μmol C, indicating that ^{18}O-GPP decreased with depth approximately twice as fast as ^{14}C-PP, which is consistent with previous observations at Station ALOHA (Quay et al. 2010). The ^{18}O-GPP to ^{14}C-PP ratio averaged 1.8 ± 0.1 in surface waters (5–45 m) and 1.3 ± 0.1 in the deeper section of the euphotic zone (75–100 m). The values and the decreasing pattern of GPP to ^{14}C-PP ratios are also consistent with previous observations at Station ALOHA (Corno et al. 2005; Juranek and Quay 2005; Quay et al. 2010).

Fig. 6 shows the depth-profiles of estimated CR and NCP based on the ^{18}O-GPP and NOC during the incubations. CR

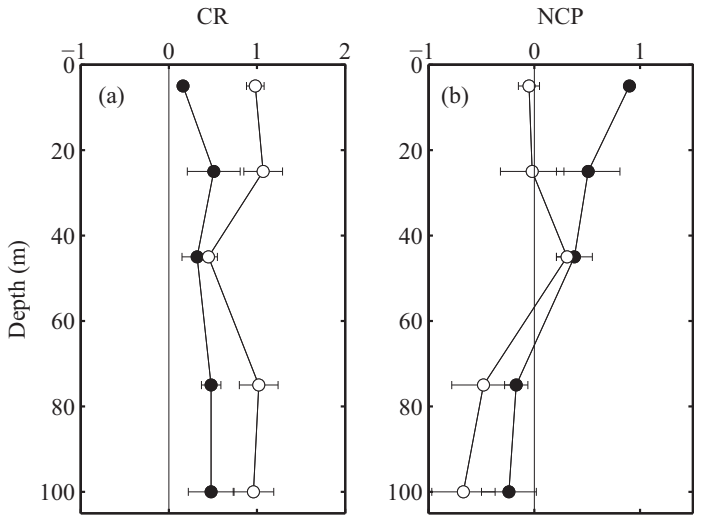

Fig. 6. Depth profiles of (a) CR and (b) NCP, both in μmol O_2 L^{-1} d^{-1} at Station ALOHA. The values are estimated from ^{18}O-GPP and NOC during the incubations (see text). Black and white circles represent profiles conducted on 07 April 2015 (HOE-Legacy 1) and 23 May 2015 (HOT 272), respectively.

Table 4. Depth integrated values of ^{18}O-GPP, ^{14}C-PP, CR, and NCP for the two in situ experiments conducted at Station ALOHA.

	07 April 2015	23 May 2015	Units
^{18}O-GPP	66 ± 2	72 ± 3	mmol O_2 m^{-2} d^{-1}
^{14}C-PP	37 ± 2	47 ± 1	mmol C m^{-2} d^{-1}
CR	40 ± 8	87 ± 10	mmol O_2 m^{-2} d^{-1}
NCP	26 ± 8	−15 ± 13	mmol O_2 m^{-2} d^{-1}
^{18}O-GPP/^{14}C-PP	1.8 ± 0.2	1.6 ± 0.1	mol O_2/mol C

values ranged from 0.2 μmol O_2 L^{-1} d^{-1} to 1.1 μmol O_2 L^{-1} d^{-1}. These values are within the range previously reported at Station ALOHA (Martínez-García and Karl 2015; Williams et al. 2004). The median variability associated with these estimates, calculated by propagating the SD of ^{18}O-GPP and NOC measurements, was ± 22%. The resulting NCP values ranged between −0.7 and 0.9 μmol O_2 L^{-1} d^{-1} (Fig. 6b), but in this case the median of the associated variability was ± 61%.

Trapezoidal integration was used to calculate depth integrated rates of ^{18}O-GPP, ^{14}C-PP, CR, and NCP from the two profiles conducted at Station ALOHA (Table 4). The ^{18}O-GPP values for the top 100 m of the water column are well within the range of previously reported values (Juranek and Quay 2005; Quay et al. 2010). We observed an increase in ^{18}O-GPP (0–100 m) from the HOE-Legacy 1 profile to the one conducted during HOT 272 of approximately 11%, while the CR (0–100 m) showed a twofold increase. This increase in CR appeared to be the cause of the large difference of integrated NCP between both profiles (from +26 to −15 mmol O_2 m^{-2} d^{-1}).

For HOE-Legacy 1, the NOC values in the treatments with and without the addition of ^{18}O-H_2O were not significantly different. However, for surface depths (0–45 m) the NOC values in the bottles with added ^{18}O-H_2O were on average 0.4 μmol O_2 L^{-1} d^{-1} greater than in the treatment with no addition of ^{18}O-H_2O. The depth-integrated CR and NCP calculated using the NOC derived from the treatment with no ^{18}O-H_2O added would result in 79 ± 20 and −13 ± 23 mmol O_2 m^{-2} d^{-1}, respectively (instead of 40 ± 8 and 26 ± 8 mmol O_2 m^{-2} d^{-1}, respectively). Therefore, even if the treatments were not significantly different, the resulting integrated CR and NCP values using the two different treatments differed substantially.

In summary, the ^{18}O-GPP profiles presented here demonstrate that, even in a low productivity oceanic region such as the North Pacific Subtropical Gyre, it is possible to precisely measure ^{18}O-GPP throughout the top 100 m of the water column using MIMS. Potentially, one can simultaneously derive CR and NCP values in the same incubation bottles, but these estimates are associated with large variability and are based on the assumption that respiration does not vary throughout the day, and that photosynthesis and respiration are the only processes affecting dissolved O_2 concentrations during the incubation. Both assumptions have been challenged before (Pamatmat 1997; Church et al. 2004; Kitidis et al. 2014). In addition, although not significant, we observed larger NOC in bottles with added ^{18}O-H_2O compared to those with no addition, which substantially changes the resulting depth integrated CR and NCP values.

Diel variability in ^{18}O-GPP

The ^{18}O in vitro method can also be applied in short incubations to investigate diel changes in GPP, due mostly to changes in solar irradiance, internal clocks and/or physiology of phytoplankton. As an example, ^{18}O-GPP was measured during 3-h incubations at different times of the day during the HOE-Legacy 1 cruise. The incubations were conducted in 60-mL glass bottles with ground-glass stoppers, inside a flow-through incubator that mimicked the light level at 25 m depth. For the first incubation (7:00 to 10:00, local time), the seawater was collected directly from the rosette into the incubation bottles following the procedure described in the Materials and procedures section. For that same cast, seawater was collected into three acid-washed 4-L polycarbonate bottles that were maintained inside the on-deck incubator until the time of the following incubation. At the time of each incubation, triplicate time-zero and incubation samples were subsampled by siphoning from one of the polycarbonate bottles into glass vials. The incubation time periods were: 7:00–10:00, 10:00–13:00, 13:00–16:00, and 16:00–19:00 h, local time.

Fig. 7 shows the hourly ^{18}O-GPP rates from the 3-h incubations started at different times of the day. Measured ^{18}O-GPP values in the different incubations were significantly different ($p < 0.01$). Mean ^{18}O-GPP values varied from 0.11 ± 0.01 μmol O_2 L^{-1} h^{-1} in the 16:00 to 19:00 incubation to 0.17 ± 0.02 μmol O_2 L^{-1} h^{-1}, in the 13:00 to 16:00 incubation. The time integrated ^{18}O-GPP from 7:00 to 19:00 resulted in 0.57 ± 0.02 μmol O_2 L^{-1} d^{-1}. These results are yet another example of the versatility of the ^{18}O in vitro method using MIMS.

Inter-comparison between IRMS and MIMS to measure ^{18}O-GPP

In order to validate the use of MIMS to measure ^{18}O-GPP via the in vitro ^{18}O method we conducted an inter-comparison experiment, in which parallel ^{18}O-GPP samples were measured via MIMS and IRMS. Seawater was collected in an acid-washed 20-L carboy from 25 m during HOT 274 (July 2015) from the HOT Station Kaena (21 50.8′ N, 158 21.8′ W). The seawater was maintained in the dark at near in situ temperature overnight, until arrival to the laboratory. Once in the lab, the seawater was siphoned into ten acid-washed Wheaton 300-mL glass bottles with ground-glass stoppers, spiked with 1650 μL of ^{18}O-H_2O to a final average enrichment of 2676 ± 20‰ (±SD), and incubated at 26°C for 6 h in an outside incubator that mimics the ocean light field at 25 m. Immediately after the incubation was started, time zero-quadruplicate samples were collected for each method by siphoning from the carboy. Once the incubation was finished, subsamples for MIMS and IRMS analysis were siphoned from the same incubation bottle. Samples for MIMS analysis were siphoned into 40 mL glass serum vials, overfilling at least twice the volume of the bottle, crimped sealed, and fixed with mercuric chloride. Samples for IRMS were collected into pre-poisoned pre-evacuated glass flasks as described in the Materials and procedures section.

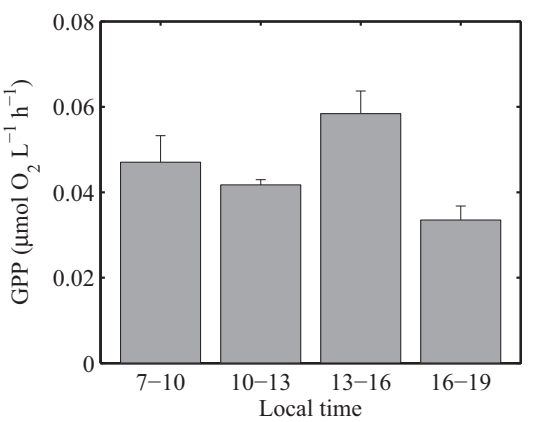

Fig. 7. Hourly ^{18}O-GPP rates for 3-h incubations conducted at different times of the day. The bars and error bars represent the mean and one SD of triplicate samples, respectively.

Results from the inter-comparison are presented in Table 5. The mean $\delta^{18}O(O_2)$ values relative to the time zero measured by MIMS were on average 0.3‰ smaller than those measured by IRMS. This difference is within the MIMS precision for $\delta^{18}O(O_2)$ measurements (±0.4‰). Despite this difference and the narrow range of values compared, the ^{18}O-GPP values measured by both techniques were significantly correlated ($r^2 = 0.47$), and agreed to within 0.02 μmol O_2 L^{-1}, which is comparable to the variability observed within the replicates for both methods (Table 5) and to the uncertainty estimated for ^{18}O-GPP measured by MIMS using a similar enrichment (Table 2). Hence, we conclude that the good agreement between both techniques justifies using MIMS to determine ^{18}O-GPP using the in vitro ^{18}O method.

Discussion

The results presented here demonstrate that the MIMS system described provides a precise, simple, and affordable way to measure in vitro ^{18}O-GPP in the ocean, and likewise, other aquatic ecosystems. Although the method does not reach the

Table 5. Comparison of ^{18}O-GPP measured by MIMS and by IRMS. Units for $\delta^{18}O(O_2)$ and ^{18}O-GPP are ‰ and μmol O_2 L^{-1}, respectively. The duration of the incubation was 6.25 h. The last column is the deviation calculated as the difference between ^{18}O-GPP measured by MIMS and ^{18}O-GPP measured by IRMS in μmol O_2 L^{-1}.

Bottle	$\delta^{18}O(O_2)_{MIMS}$	$^{18}O\text{-}GPP_{MIMS}$	$\delta^{18}O(O_2)_{IRMS}$	$^{18}O\text{-}GPP_{IRMS}$	$\Delta^{18}O\text{-}GPP_{MIMS\text{-}IRMS}$
1	7.4	0.61	7.3	0.60	0.01
2	7.2	0.58	7.5	0.61	−0.03
3	7.0	0.57	7.6	0.62	−0.05
4	7.1	0.58	7.3	0.59	−0.01
5	7.5	0.62	7.6	0.63	−0.01
6	7.3	0.60	7.5	0.61	−0.01
7	6.7	0.55	6.9	0.57	−0.02
8	7.2	0.60	7.5	0.62	−0.02
9	6.6	0.55	7.2	0.59	−0.04
10	6.9	0.56	7.4	0.60	−0.04
Mean±SD	7.1 ± 0.3	0.58 ± 0.02	7.4 ± 0.2	0.60 ± 0.02	−0.02 ± 0.02

precision of an IRMS system for $\delta^{18}O(O_2)$ analysis ($\pm 0.4‰$ for MIMS compared to $\pm 0.1‰$ for IRMS), and therefore is not suitable for the analysis of the $\delta^{18}O$ of ambient dissolved O_2 as an in situ tracer for biological productivity (Quay et al. 1993), the measurements are precise enough to detect biological changes of $\delta^{18}O(O_2)$ in $H_2^{18}O$-enriched samples, even in a low productivity environment such as the North Pacific Subtropical Gyre and with initial water enrichments as low as ~400‰ (Fig. 3; Table 2). The method has been applied successfully for incubations ranging from 3 to 12 h (Figs. 4 and 7) at the oligotrophic Station ALOHA. Measured ^{18}O-GPP were correlated with ^{14}C-PP measurements (Fig. 5), and the average ^{18}O-GPP/^{14}C-PP ratio is in good agreement with previous observations at Station ALOHA (Quay et al. 2010). The addition of labeled ^{18}O-H_2O did not affect ^{14}C-PP (Table 3) or ^{18}O-GPP (Fig. 3b). Lastly, an intercomparison exercise between IRMS and MIMS showed that ^{18}O-GPP values were comparable for the two methods and agreed to within ± 4% (Table 5), which clearly validates the MIMS approach to measure in vitro ^{18}O-GPP in the ocean.

One of the advantages of the MIMS method is that the handling of the samples is easier than for the IRMS method, as there is no need to extract the gases into a head space, and therefore the likelihood of sample contamination is lessened. In addition to ease of sample handling, operation and maintenance of a MIMS system is also simple and straightforward, and it does not require that the instrument is specifically set up for the analysis of $^{18}O^{16}O$ or that is operated by highly trained personnel. Calibration of the instrument is straightforward and only requires 0.2 μm filtered seawater. The MIMS systems are relatively inexpensive, making them affordable to a number of research groups. In addition, MIMS systems are portable and have the capability of being used onboard research vessels at sea, which increases the number of measurements feasibly conducted during oceanographic cruises, while decreasing the storage time of the samples. It also provides a convenient method for near real-time estimation of GPP, NOC, and CR in shipboard incubation experiments. Sample analysis requires only ~5 min per sample. This implies that, for example, a HOT standard primary production depth profile with six depths and triplicate samples for each depth can be analyzed for ^{18}O-GPP in approximately 3–4 h, including the time zero triplicate samples. The onboard capability together with the rapid analysis time not only makes it possible to process many samples at sea, but also to obtain timely results that could potentially help with field sampling strategy decisions. A growing number of research groups capable of conducting the ^{18}O in vitro method by the application of the MIMS approach, and the high number of samples that this technique allows within a given research expedition, could potentially escalate the number ^{18}O-GPP observations and help improve the time and space distributions of oceanic GPP, and ultimately improve our understanding of the biological carbon pump. In addition to in vitro ^{18}O-GPP observations, a shipboard MIMS could be potentially used during an oceanographic cruise to analyze major dissolved gases in situ, such as O_2 and Ar, providing an incubation-free estimate of productivity (Kaiser et al. 2005; Hamme et al. 2012; Tortell et al. 2014; Ferrón et al. 2015).

Summary and recommendations

The data presented here are, to our knowledge, the first application of MIMS to measure ^{18}O-GPP in oceanic waters. In principle, any other MIMS configuration should also be suitable to measure $\delta^{18}O(O_2)$ in enriched samples, provided that it achieves similar accuracy and precision to the one described here. This approach should also be appropriate for other aquatic environments such as more productive oceanic regions, and coastal marine and freshwater aquatic environments. We have shown that in addition to ^{18}O-GPP and without the need for additional samples, it is possible to obtain information about other metabolic rates such as CR and NCP, based on the net change in O_2/Ar ratios, although these estimates are based on a number of assumptions and subjected to larger uncertainties than ^{18}O-GPP.

Because the ^{18}O in vitro method quantifies a well-defined process, gross oxygen production by splitting H_2O, ^{18}O-GPP observations are very useful to help interpret the results from other productivity measurements (Bender et al. 1987; Grande et al. 1989; Quay et al. 2010; Juranek and Quay 2012). However, as with any in vitro method, this technique is susceptible to artifacts related to incubating seawater in a confined bottle. These artifacts are most commonly related to grazer exclusion and to changes to the natural environmental conditions (e.g., temperature, light, turbulence, contamination, accumulation of excretion products) (Robinson and Williams 2005). Whenever possible, measures should be taken to minimize these artifacts. Some of these considerations include selecting an adequate sample volume, avoiding the introduction of contaminants, incubating in situ rather than inside an incubator, and using quartz bottles to avoid modifying the light spectrum.

References

Behrenfeld, M. J., and P. G. Falkowski. 1997. Photosynthetic rates derived from satellite-based chlorophyll concentration. Limnol. Oceanogr. **42**: 1–20. doi:10.4319/lo.1997.42.1.0001

Bekker, A., and others. 2004. Dating the rise of atmospheric oxygen. Nature **427**: 117–120. doi:10.1038/nature02260

Bender, M., and others. 1987. A comparison of four methods for determining planktonic community production. Limnol. Oceanogr. **32**: 1085–1098. doi:10.4319/lo.1987.32.5.1085

Bender, M., J. Orchardo, M. L. Dickson, R. Barber, and S. Lindley. 1999. In vitro O_2 fluxes compared with ^{14}C production and other rate terms during the JGOFS Equatorial Pacific experiment. Deep-Sea Res. I **46**: 637–654. doi: 10.1016/S0967-0637(98)00080-6

Church, M. J., H. W. Ducklow, and D. M. Karl. 2004. Light dependence of [^{3}H] leucine incorporation in the oligotrophic North Pacific Ocean. Appl. Environ. Microbiol **70**: 4079–4087. doi:10.1128/AEM.70.7.4079-4087.2004

Corno, G., R. M. Letelier, M. R. Abbott, and D. M. Karl. 2005. Assessing primary production variability in the North Pacific subtropical gyre: A comparison of fast repetition rate fluorometry and ^{14}C measurements. J. Phycol. **42**: 51–60. doi:10.1111/j.1529-8817.2006.00163.x

Dring, M. J., and D. H. Jewson. 1982. What does ^{14}C uptake by phytoplankton really measure? A theoretical modeling approach. Proc. R. Soc. Lond. B Biol. **214**: 351–368. doi:10.1098/rspb.1982.0016

Emerson, S., C. Stump, D. Wilbur, and P. Quay. 1999. Accurate measurement of O_2, N_2, and Ar gases in water and the solubility of N_2. Mar. Chem. **64**: 337–347. doi:10.1016/S0304-4203(98)00090-5

Eppley, R. W., and J. H. Sharp. 1975. Photosynthetic measurements in the central North Pacific: The dark loss of carbon in 24-h incubations. Limnol. Oceanogr. **20**: 981–988. doi:10.4319/lo.1975.20.6.0981

Falkowski, P. G., and J. A. Raven. 2007. Aquatic photosynthesis, 2nd ed, 500 pp. Princeton Univ. Press.

Ferrón, S., S. T. Wilson, S. Martínez-García, P. D. Quay, and D. M. Karl. 2015. Metabolic balance in the mixed layer of the oligotrophic North Pacific Ocean from diel changes in O_2/Ar saturation ratios. Geophys. Res. Lett. **42**: 3421–3430. doi:10.1002/2015GL063555

Field, C. B., M. J. Behrenfeld, J. T. Randerson, and P. Falkowski. 1998. Primary production of the biosphere: Integrating terrestrial and oceanic components. Science **281**: 237–240. doi:10.1126/science.281.5374.237

Fitzwater, S. E., G. A. Knauer, and J. H. Martin. 1982. Metal contamination and its effect on primary production measurements. Limnol. Oceanogr. **27**: 544–551. doi:10.4319/lo.1982.27.3.0544

Gaarder, T., and H. H. Gran. 1927. Investigations of the production of plankton in the Oslo Fjord. Rapp, P. v. Reun. Cons. Perm. Int. Explor. Mer **42**: 1–48.

García, H. E., and L. I. Gordon. 1992. Oxygen solubility in seawater: Better fitting equations. Limnol. Oceanogr. **37**: 1307–1312. doi:10.4319/lo.1992.37.6.1307

Grande, K. D., and others. 1989. Primary production in the North Pacific gyre: A comparison of rates determined by the ^{14}C, O_2 concentration and ^{18}O methods. Deep-Sea Res. **36**: 1621–1634. doi:10.1016/0198-0149(89)90063-0

Hamme, R. C., and S. R. Emerson. 2004. The solubility of neon, nitrogen and argon in distilled water and seawater. Deep-Sea Res. Part I **51**: 1517–1528. doi:10.1016/j.dsr.2004.06.009

Hamme, R. C., and others. 2012. Dissolved O_2/Ar and other methods reveal rapid changes in productivity during a Lagrangian experiment in the Southern Ocean. J. Geophys. Res. **117**: C00F12. doi:10.1029/2011JC007046

Juranek, L. W., and P. D. Quay. 2005. In vitro and in situ gross primary and net community production in the North Pacific Subtropical Gyre using labeled and natural abundance isotopes of dissolved O_2. Global Biogeochem. Cycles **19**: GB3009. doi:10.1029/2004GB002384

Juranek, L. W., and P. Quay. 2012. Using triple isotopes of dissolved oxygen to evaluate global marine productivity. Annu. Rev. Mar. Sci. **5**: 503–524. doi:10.1146/annurev-marine-121211-172430

Kaiser, J., M. K. Reuer, B. Barnett, and M. L. Bender. 2005. Marine productivity estimates from continuous O_2/Ar ratio measurements by shipboard membrane inlet mass spectrometry. Geophys. Res. Lett. **32**: L19605. doi:10.1029/2005GL023459

Kana, T. M., C. Darkangelo, M. D. Hunt, J. B. Oldham, G. E. Bennett, and J. C. Cornwell. 1994. Membrane inlet mass spectrometer for rapid high-precision determination of N_2, O_2, and Ar in environmental water samples. Anal. Chem. **66**: 4166–4170. doi:10.1021/ac00095a009

Kana, T. M., J. C. Cornwell, and L. Zhong. 2006. Determination of denitrification in the Chesapeake Bay from measurements of N_2 accumulation in bottom water. Estuaries Coast **29**: 222–231. doi:10.1007/BF02781991

Karl, D. M. 2014. Solar energy capture and transformation in the sea. Elem. Sci. Anth. **2**: 000021. doi:10.12952/journal.elementa.000021

Karl, D. M., and R. Lukas. 1996. The Hawaii Ocean Time-series (HOT) program: Background, rationale and field implementation. Deep-Sea Res. II **43**: 129–156. doi:10.1016/0967-0645(96)00005-7

Karl, D. M., and others. 1996. Seasonal and interannual variability in primary production and particle flux at Station ALOHA. Deep-Sea Res. Part II **43**: 539–568. doi:10.1016/0967-0645(1096)00002-1

Karl, D. M., D. V. Hebel, K. Björkman, and R. M. Letelier. 1998. The role of dissolved organic matter release in the productivity of the oligotrophic North Pacific Ocean. Limnol. Oceanogr. **43**: 1270–1286. doi:10.4319/lo.1998.43.6.1270

Karl, D. M., and M. J. Church. 2014. Microbial oceanography and the Hawaii Ocean Time-series programme. Nat. Rev. Microbiol. **12**: 699–713. doi:10.1038/nrmicro3333

Kitidis, V., G. H. Tilstone, P. Serret, T. J. Smyth, R. Torres, and C. Robinson. 2014. Oxygen photolysis in the Mauritanian upwelling: Implications for net community production. Limnol. Oceanogr. **59**: 299–310. doi:10.4319/lo.2014.59.2.0299

Kroopnick, P., and H. Craig. 1972. Atmospheric oxygen: Isotopic composition and solubility fractionation. Science **175**: 54–55. doi:10.1126/science.175.4017.54

Marra, J. 2002. Approaches to the measurement of plankton production, p. 222–264. *In* P. J. l. Williams, D. N. Thomas and C. S. Reynolds [eds.], Phytoplankton productivity: Carbon assimilation in marine and freshwater ecosystems. Blackwell Science Ltd. doi:10.1002/9780470995204.ch4

Martínez-García, S., and D. M. Karl. 2015. Microbial respiration in the euphotic zone at Station ALOHA. Limnol. Oceanogr. **60**: 1039–1050. doi:10.1002/lno.10072

McKinney, C. R., J. M. McCrea, S. Epstein, H. A. Allen, and H. C. Urey. 1950. Improvements in mass spectrometers for the

measurement of small differences in isotope abundance ratios. Rev. Sci. Instrum. **21**: 724–730. doi:10.1063/1.1745698

Pamatmat, M. M. 1997. Non-photosynthetic oxygen production and non-respiratory oxygen uptake in the dark: A theory of oxygen dynamics in plankton communities. Mar. Biol. **129**: 735–746. doi:10.1007/s002270050216

Pei, S., and E. A. Laws. 2014. Does the ^{14}C method estimate net photosynthesis? II. Implications from cyclostat studies of marine phytoplankton. Deep-Sea Res. I **91**: 94–100. doi:10.1016/j.drs.2014.05.015

Peterson, B. J. 1980. Aquatic primary productivity and the ^{14}C-CO_2 method: A history of the productivity problem. Annu. Rev. Ecol. Syst **11**: 359–385. doi:10.1146/annurev.es.11.110180.002043

Quay, P. D., S. Emerson, D. O. Wilbur, C. Stump, and M. Knox. 1993. The $\delta^{18}O$ of dissolved O_2 in the surface waters of the subarctic Pacific: A tracer of biological productivity. J. Geophys. Res. **98**: 8447–8458. doi:10.1029/92JC03017

Quay, P. D., C. Peacock, K. Björkman, and D. M. Karl. 2010. Measuring primary production rates in the ocean: Enigmatic results between incubation and non-incubation methods at Station ALOHA. Global Biogeochem. Cycles **24**: GB3014. doi:10.1029/2009GB003665

Regaudie-de-Gioux, A., S. Lasternas, S. Agustí, and C. M. Duarte. 2014. Comparing marine primary production estimates through different methods and development of conversion equations. Front. Mar. Sci. **1**: 1–14. doi:10.3389/fmars.2014.00019

Robinson, C., and P. J. L. Williams. 2005. Respiration and its measurement in the surface waters, p. 147–180. *In* P. A. Del Giorgio and P. J. l. Williams [eds.], Respiration in aquatic ecosystems. Oxford Univ. Press. doi:10.1093/acprof:oso/9780198527084.003.0009

Ryther, J. H. 1955. The ratio of photosynthesis to respiration in marine plankton algae an its effect upon the measurement of productivity. Deep-Sea Res **2**: 134–139. doi:10.1016/0146-6313(55)90015-0

Ryther, J. H. 1969. Photosynthesis and fish production in the sea. Science **166**: 72–76. doi:10.1126/science.166.3901.72

Steemann Nielsen, E. 1952. The use of radioactive carbon (C^{14}) for measuring organic production in the sea. J. Cons. Int. Explor. Mer **18**: 117–140. doi:10.1093/icesjms/18.2.117

Tortell, P. D., and others. 2014. Metabolic balance of coastal Antartic waters revealed by autonomous pCO_2 and ΔO_2/Ar measurements. Geophys. Res. Lett. **41**: 6803–6810. doi:10.1002/2014GL061266

Viviani, D. A., D. M. Karl, and M. J. Church. 2015. Variability in photosynthetic production of dissolved and particulate organic carbon in the North Pacific Subtropical Gyre. Front. Mar. Sci. **2**: 73. doi:10.3389/fmars.2015.00073

Volk, T., and M. I. Hoffer. 1985. Ocean carbon pumps: Analysis of relative strengths and efficiencies in ocean-driven atmospheric CO_2 changes, p. 99–110. *In* E. T. Sundquist and W. S. Broecker [eds.], The carbon cycle and atmospheric CO_2: Natural variations archean to present. American Geophysical Union, Washington D. C., doi:10.1029/GM032p0099

Westberry, T., M. J. Behrenfeld, D. A. Siegel, and E. Boss. 2008. Carbon-based primary productivity modeling with vertically resolved photoacclimation. Global Biogeochem. Cycles **22**: GB2024. doi:10.1029/2007GB003078

Williams, P. J. L., and D. A. Purdie. 1991. *In vitro* and *in situ* derived rates of gross production, net community production and respiration of oxygen in the oligotrophic subtropical gyre of the North Pacific Ocean. Deep-Sea Res. **38**: 891–910. doi:10.1016/0198-0149(91)90024-A

Williams, P. J. L., P. J. Morris, and D. M. Karl. 2004. Net community production and metabolic balance at the oligotrophic ocean site, station ALOHA. Deep-Sea Res. I **51**: 1563–1578. doi:10.1016/j.dsr.2004.07.001

Acknowledgments

We thank the captain and crew of the R.V. *Kilo Moana* for their assistance in field operations. Thanks to Abby Bate, Tara Clemente, and Eric Shimabukuro for help in sample collection, Johnny Stutsman for sample analysis by IRMS, Todd N. Kana for helpful discussion, and the Hawaii Ocean Time-series (HOT) team that facilitated part of this work. The manuscript benefited from the input of two anonymous reviewers. This research was supported by the National Science Foundation (NSF) through the Center for Microbial Oceanography: Research and Education (C-MORE; EF04-24599 to D.M.K.), the Hawaii Ocean Time-series program (OCE12-60164 to M.J.C. and D.M.K.), the Gordon and Betty Moore Foundation (D.M.K., #3794), and the Simons Collaboration on Ocean Processes and Ecology (SCOPE). S. F. was funded by a C-MORE fellowship and for a portion of this period by the Balzan Prize for Oceanography (awarded to D.M.K.). Data are freely available at http://hahana.soest.hawaii.edu/cmoreDS/interface.html and upon request.

Submitted 12 February 2016
Revised 14 May 2016
Accepted 19 May 2016

Associate editor: Tammi Richardson